EUROPHYSICS LETTERS 15 April 2006

Europhys. Lett., **74** (2), pp. 362–368 (2006)
DOI: 10.1209/epl/i2005-10519-x

Turbulent drag reduction by surfactants

J. Drappier[1], T. Divoux[1], Y. Amarouchene[1,2], F. Bertrand[3], S. Rodts[3], O. Cadot[4], J. Meunier[1] and Daniel Bonn[1,5](*)

[1] *Ecole Normale Supérieure, Laboratoire de Physique Statistique*
24 rue Lhomond, 75231 Paris Cedex 05, France
[2] *Centre de Physique Moléculaire Optique et Hertzienne*
351 cours de la Libération, 33405 Talence, France
[3] *LMSGC, ENPC - 6-8 avenue Blaise Pascal*
77455 Marne-la-Vallée Cedex 2, France
[4] *Université du Havre, Laboratoire de mécanique*
25 rue Philippe Lebon, 76600 Le Havre, France
[5] *van der Waals-Zeeman Institute - Valckenierstraat 65*
1018 XE Amsterdam, the Netherlands

received 29 September 2005; accepted in final form 14 February 2006
published online 10 March 2006

PACS. 83.60.Yz – Drag reduction.
PACS. 82.70.Uv – Surfactants, micellar solutions, vesicles, lamellae, amphiphilic systems (hydrophilic and hydrophobic interactions).
PACS. 83.50.Rp – Wall slip and apparent slip.

Abstract. – Drag reduction of turbulent flows by surfactant additives is studied. The surfactant forms a shear-induced gel phase in both rheological and turbulent flows. In both flows, the fracture of the gel causes an apparent wall slip. The slipping in turbulent flows decreases the wall friction and therefore immediately leads to drag reduction, providing a detailed mechanism for drag reduction by surfactants.

Introduction. – A spectacular reduction of energy losses in turbulent flows can be achieved by the addition of small amounts of certain polymers or surfactants [1, 2]. For polymers, drag reduction is due to the large elongational viscosity of the polymer solution; this stabilizes the turbulent boundary layer, leading to less turbulent energy generation, and hence less dissipation [3, 4]. For surfactants, the phenomenon is still ill understood, in spite of the enormous attention the subject attracted over the past few decades, and the fact that due to their reversible degradation of the aggregates, surfactant solutions are better adapted to industrial applications than polymers that degrade irreversibly [5]. Surfactant drag reduction is uniquely found for systems forming wormlike micelles. These micelles are self-assembled structures in which the surfactants form tubular structures with a diameter roughly twice the size of a surfactant molecule and a length that can be thousands of times the molecular size. The flow behavior of dilute solutions of such wormlike micelles in both laminar and turbulent

(*) E-mail: bonn@lps.ens.fr.

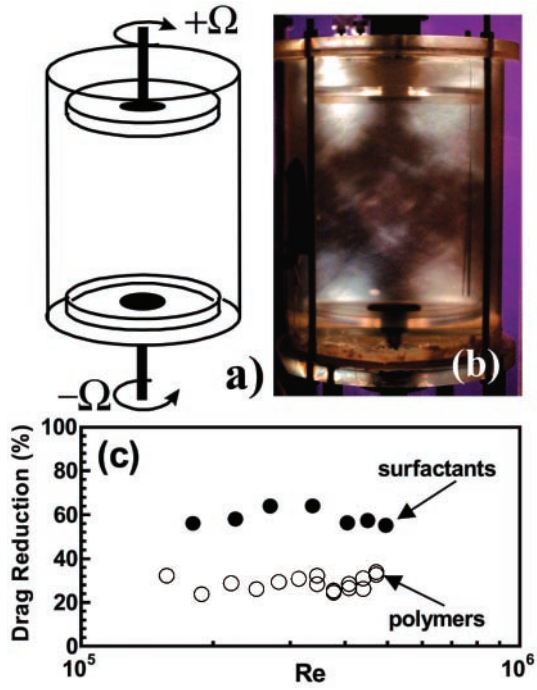

Fig. 1 – (a) The turbulence cell used for the measurements. (b) The shear-induced birefringent gel in the turbulent boundary layer observed by visualization between crossed polarizers. (c) Drag reduction for polymer and surfactant solutions measured at different Reynolds numbers.

flows can be very different from that of the solvent alone, even at very low concentrations of surfactant [2, 6, 7].

The mechanism of turbulent drag reduction by surfactants was long believed to be similar to that of polymers, implying that the phenomenon is due to a high elongational viscosity. Some studies on drag-reducing surfactants confirm the correlation of high apparent extensional viscosity with drag reduction [8], however others claim that its importance is minor [2(a)]. In this letter we show that drag reduction of surfactant solutions is due to an effective wall slip. This effective wall slip, in turn, is due to the formation of a shear-induced "gel" that can break in the near-wall region. Due to the effective wall slip, the bulk of the turbulent system does not experience a large wall friction. Since it is the wall friction that generates the turbulence, this naturally leads to a smaller dissipation. A measurement of the elongational viscosity η_e shows that, although η_e can be important for drag-reducing surfactant solutions, the breakage of the gel also happens in elongational flows, and leads to very low elongational viscosities.

Experimental. – The surfactant solution we used for most of the experiments described here is made with 0.5 wt% of CTAB (cetyltrimethyl ammonium bromide) and 0.1 wt% of NaSal (sodium salycilate), both from Sigma in ultra pure water. The overlap concentration c^* giving the crossover between dilute and semi-dilute solutions was determined from viscosity measurements to be at 1.2 wt% CTAB for this CTAB/NaSal ratio. All of the measurements (with the exception of some of those shown in fig. 4 below) were thus done in the dilute regime. To check the generality of our conclusions, a number of other drag-reducing surfactants were tested: CTAC/salicylate, CPCL/salycilate (0.06 M/0.12 M) [2, 6, 9] and the industrial

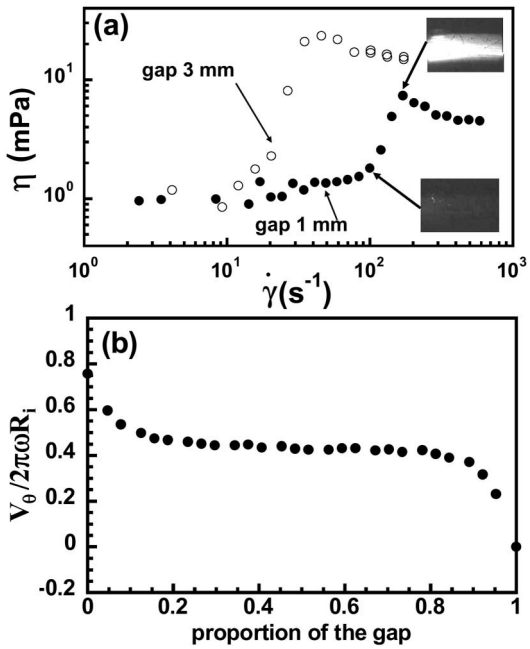

Fig. 2 – (a) Viscosity of the surfactant solution measured in a Couette cell: two concentric cylinders spaced by 1 mm or 3 mm. Inset: visualization in the gap between crossed polarizers; the fluid becomes birefringent at the viscosity increase. (b) The orthoradial velocity profile measured by MRI in the Couette cell; R_i is the radius of the rotating inner cylinder.

drag-reducing surfactants Habon-G (10 wppm) [10] and Ethoquad T13/27W/salycilate [8] at 200 wppm and a 2 : 1 molar ratio of salt to surfactant. All these show qualitatively the same behavior as the CTAB/NaSal system in both rheological and turbulent flows.

The rheology is done using a stress-controlled commercial rheometer (Reologica Stress-Tech). The viscosity of the surfactant solution is measured using two different gap Couette cells (two concentric cylinders the inner of which is turning); the gaps for the two different cells are 1 mm or 3 mm.

The turbulence is generated in a closed cylindrical cell between two counter-rotating disks at a constant angular velocity Ω, spaced one disk-diameter apart (fig. 1). The integral Reynolds number is $\mathrm{Re} = \Omega R^2/\nu$, where R is the radius of the disks and ν the kinematic viscosity of water.

We measure the elongational viscosity η_e for the surfactants by looking at droplet fission with a rapid camera; the dynamics of the thinning of the filament (notably its minimum thickness h_min) that connects the droplet to the orifice can be used to obtain the elongational viscosity η_e [11]. We therefore film the droplet fission process using a rapid camera at a frame rate of a 1000 images/s. The dynamics of the thinning of the filament can be used to obtain the elongational viscosity: $\eta_\mathrm{e} = 2\gamma/(h_\mathrm{min}\dot{\varepsilon})$, where h_min is the radius, γ the surface tension and $\dot{\varepsilon}$ the elongation rate defined as $-2(\mathrm{d}h_\mathrm{min}/\mathrm{d}t)/h_\mathrm{min}$.

Results. – Figure 2a shows the measured flow curves. In the rheology, the dilute wormlike micelles show a pronounced shear-thickening behavior (*i.e.*, a viscosity increase with increasing velocity gradient), followed by an equally pronounced shear thinning, as reported previously in [2,6,9]. The results are different for different gaps; this dependence on the gap indicates an

apparent wall slip. The apparent wall slip velocity in the rheology experiments can be deduced directly in the rheological measurements. Imposing the stress in the experiments, and using

$$\dot{\gamma}_{\text{apparent}} = \dot{\gamma}_{\text{real}} + \frac{2v_{\text{slip}}}{b}$$

with b the gap of the Couette cell, from the difference in apparent shear rate for two different gaps of the Couette cell at the same stress the wall slip velocity can be calculated. This will be used below to compare with the amount of drag reduction. An interesting observation in the rheology experiments for which we have no explanation at present is that for even smaller gaps (0.125 mm) the shear thickening disappears altogether.

Birefringence measurements under flow show that the viscosity increase is due to the formation of a new and highly birefringent phase (fig. 2a); because of its appearance and high viscosity, we call this shear-induced structure (SIS) phase a "gel" [6]. However, it should be kept in mind that usually the term gel denotes networks of cross-linked polymers; our shear-induced phase is likely to be much more complicated than that [6]. A direct measurement of the orthoradial velocity profile in the gap of a Couette cell using Magnetic Resonance Imaging (MRI) [12] shows that all the shear is concentrated in a small region near the walls (fig. 2b). This is the origin of the apparent wall slip in the rheology measurements, which therefore is indeed only apparent. The most likely explanation for these (time-averaged) velocity profiles is a repeated fracture of the shear-induced gel in the near-wall region.

For the turbulence measurements, the difference between the injected motor power between water and the surfactant solution or polymer solution gives drag reduction as: $DR = (P_{\text{water}} - P_{\text{surfactant}})/P_{\text{water}}$ *100%. In our turbulence setup, very small amounts of such micelles lead to a 60% decrease of the turbulent energy dissipation, whereas a typical drag-reducing polymer (50 wppm of Polyethylene oxide of mass $M = 4 \cdot 10^6$ gram/mole) shown for comparison gives only a 30% drag reduction (fig. 1c), which is close to the maximum drag reduction that can be achieved for polymers in this geometry [13]. For the surfactant system, the shear-induced birefringent gel also forms in the *turbulent* boundary layer. This can be observed directly by visualizing the turbulence cell between crossed polarizers. As soon as the disks are brought into movement, a highly birefringent phase forms in their immediate vicinity (fig. 1b). That the boundary layers create the turbulence in the bulk is also obvious from the visualization. We observe boundary layer instabilities that lead to ejection of the birefringent phase from this region into the turbulent bulk, leading, after several seconds, to a very heterogeneously birefringent turbulent system.

"Instantaneous" MRI measurements of the orthoradial velocity in the Couette cell for a turbulent flow (time resolution approximately 0.1 s and $\text{Re} = 5 \cdot 10^4$, defined as above with R the gap of the Couette cell) suggest that an effective wall slip may also occur when the flow is turbulent. The MRI data show that for water and the polymer solution of fig. 1 the fluid is very turbulent: the r.m.s. velocity fluctuation is 22.1 cm/s for water, and 17.9 cm/s for the polymer solution. In contrast, for the surfactants the turbulence is almost completely suppressed, because the moving wall hardly provides any drag on the bulk of the micellar solution: the r.m.s. velocity fluctuation is only 3.8 cm/s. This underlines once more that the mechanisms of drag reduction are different for surfactants and polymers: the turbulence intensity is much smaller for the surfactants than for both pure water and for the polymer solution, and indeed the surfactants give more drag reduction than the polymers.

The elongational viscosity η_{e} can be measured for the surfactants by looking at droplet fission (fig. 3(a)). We find that η_{e} is so low that the dynamics of the filament is indistinguishable from that of pure water (fig. 3(a)) for which $\eta_{\text{e}} = 3\,\text{mPa s}$: the scaling $h_{\min} \sim (t_{\text{c}} - t)^{2/3}$ reveals a simple balance between capillarity and inertia as typically observed for low viscous fluids [14].

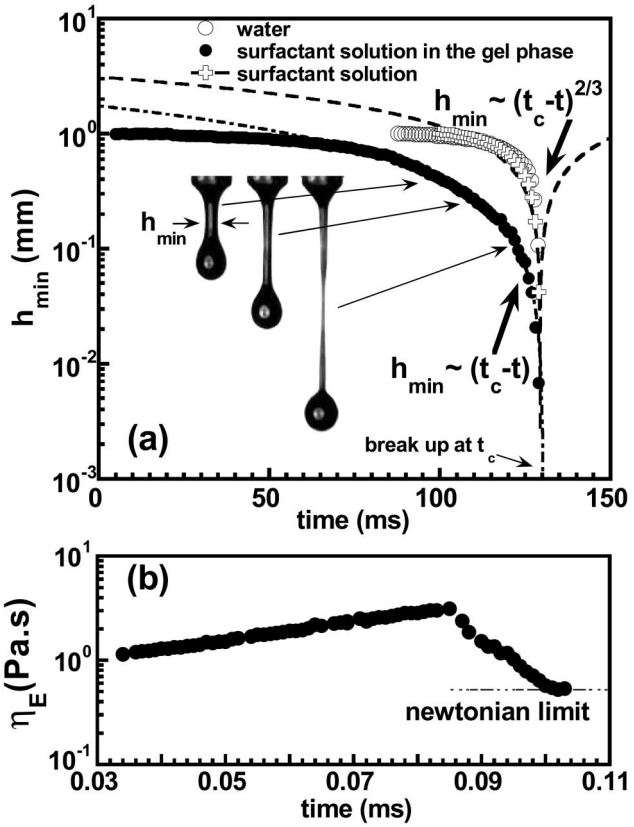

Fig. 3 – (a) Droplet fission filmed by a rapid camera. The time between each image is 1 ms. The thinning of the filament (minimum thickness $h_{\min}$) that connects the droplet to the orifice *vs.* time. (b) The elongational viscosity.

However, η_e is high (and comparable to that of typical drag-reducing polymers) if measured on the gel: if a droplet of a presheared solution detaches, a long filament forms (fig. 3(a)) that allows to quantify the elongational viscosity by a simple force balance on the filament [11].

We find that η_e of the gel increases exponentially in time during the initial stages (fig. 3), very similarly to what is observed for polymers for which growing elastic stresses must be taken into account [11]. However, the important difference is that late times (*i.e.*, at large deformations) η_e suddenly decreases rapidly, to give rise to an almost Newtonian behavior of the fluid in the filament as suggested by the linear scaling $h_{\min} \sim \gamma/\eta(t_c - t)$ that exhibits characteristics of the self-similar solution resulting from a balance between capillarity and viscosity [12]. This suggests that the shear-induced gel breaks when deformed too much.

Discussion. – The rheology thus shows that a shear-induced gel may form, with a high elongational viscosity; the gel breaks at too large deformations, causing an apparent slip at the wall. The rupture of the gel in elongational flow is compatible with the apparent wall slip observed in the simple shear flow of the Couette cell. Shear-induced gelation in similar extremely dilute solutions of wormlike micelles followed by a fracture of the gel that can lead to an apparent wall slip has been observed previously in rheological flows [6, 9]. We show here that the shear-induced gel also forms in the turbulent boundary layer, and can

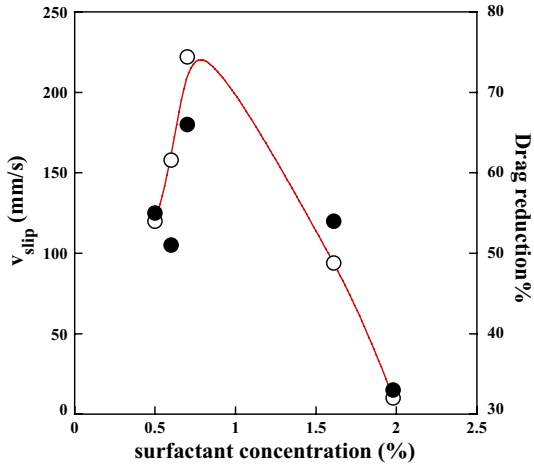

Fig. 4 – Apparent wall slip velocity (filled symbols) and drag reduction (open symbols) as a function of surfactant concentration for the CTAB/salycilate system at fixed surfactant/salt ratio.

lead to an effective wall slip there, too. Although not interpreted as such, recent precise measurements of the velocity profile in pipe flow for drag-reducing surfactants are compatible with the observations made here: the velocity does not extrapolate to zero at the wall, but to a finite value, again suggestive of an effective wall slip [2, 15]. Other measurements of the velocity profile [2, 5, 10, 16] also indicate that the near-wall velocity profile is much steeper when drag-reducing surfactants act.

The data consequently suggest that the shear-induced phase induces an effective wall slip in turbulent flows. The bulk of the fluid experiences only a small drag from the wall, and therefore the turbulence intensity is much smaller; this naturally leads to a small dissipation, since less turbulent energy is injected into the bulk by the boundary layers. In fact, the wall friction and energy dissipation are proportional to each other, and therefore, the ratio of the wall friction with and without additives equals the ratio of energy dissipation with and without additives. Consequently, the apparent wall slip directly leads to drag reduction. The possible increase in shear viscosity in the bulk, on the other hand, should not influence the total drag; as already noted by Kolmogorov, the shear viscosity does not influence the total energy dissipation, but merely fixes the length scale at which the dissipation takes place [13].

These observations provide a handle for controlling drag reduction by surfactants. By changing the surfactant concentration, the slip velocity at the wall, the pertinent quantity to describe the drag reduction ability, changes considerably (and nonlinearly) with concentration. Figure 4 depicts the drag reduction and apparent wall slip velocity (as deduced from the rheology measurements in *laminar* flow) as a function of the surfactant concentration. These follow exactly the same trend, underlining also once more that the apparent wall slip is at the origin of the drag reduction. For all other systems tested, an apparent wall slip in the rheology was observed, together with an important level of drag reduction: up to 80% for Ethoquad, thus underlining the generality of our observations.

The apparent wall slip also provides a perfectly plausible explanation of the hitherto ill-understood "pipe diameter effect". For surfactants, drag reduction depends not only on the Reynolds number but also on the diameter of the pipe [16]: in this way different amounts of drag reduction can be found for different pipe diameter but at the same Reynolds number. This pipe diameter effect is observed for surfactant solutions [16] but not for polymer solutions,

in line with the arguments presented here. Finally, our birefringence observations provide a direct visualization of the way turbulence is generated by the boundary layer, a matter that is at the heart of the turbulence problem.

* * *

We thank J. Zakin and Y. Zhang for helpful discussions. LPS de L'ENS is UMR 8550 of the CNRS, associated with the universities Paris 6 and Paris 7. CPMOH is UMR 5798 of the CNRS associated with the University Bordeaux 1.

REFERENCES

[1] Toms B. A., *Proceedings of the 1st International Rheology Congress* (North-Holland, Amsterdam) 1948.
[2] (a) Gyr A. and Bewersdorff H.-W., *Drag Reduction of Turbulent Flows by Additives* (Kluwer Academic Publishers, The Netherlands) 1995; (b) Bonn D. *et al.*, *J. Phys. Condens. Matter*, **17** (2005) S1195; L'vov V. S., Pomyalov A., Procaccia I. and Tiberkevich V., *Phys. Rev. Lett.*, **92** (2004) 244503.
[3] Landhal M. T., *Phys. Fluids*, **20** (1977) 55.
[4] Wagner C., Amarouchene Y., Doyle P. and Bonn D., *Europhys. Lett.*, **64** (2003) 823.
[5] Zakin J. L., Lu B. and Bewersdorff H. V., *Rev. Chem. Eng.*, **14** (1998) 255.
[6] Rehage H., Wunderlich I. and Hoffman H., *Prog. Colloid Polym. Sci.*, **72** (1986) 51; Liu C. H. and Pine D. J., *Phys. Rev. Lett.*, **77** (1996) 2121; for a recent proposal on the gel structure, see Cates M. E. and Candau S., *Europhys. Lett.*, **55** (2001) 887.
[7] Cates M. E., *Macromolecules*, **20** (1989) 2289; *J. Phys. Condens. Matter*, **8** (1996) 1185; Lequeux F., *Curr. Opin. Colloid Interface Sci.*, **1** (1996) 341.
[8] Lu B. *et al.*, *Langmuir*, **14** (1998) 8.
[9] Hu Y. T., Boltenhagen P., Mattys W. and Pine, *J. Rheol.*, **42** (1998) 1185.
[10] Hetsroni G., Zakin J. L. and Mosyak A., *Phys. Fluids*, **9** (1997) 2397.
[11] Amarouchène Y., Bonn D., Meunier J. and Kellay H., *Phys. Rev. Lett.*, **86** (2001) 3558.
[12] Callaghan P. T., *Rheo-NMR, Rep. Prog. Phys.*, **62** (1999) 599.
[13] Cadot O., Bonn D. and Douady S., *Phys. Fluids A*, **10** (1998) 429.
[14] Eggers J., *Rev. Mod. Phys.*, **69** (1997) 865.
[15] Li P. W., Kawaguchi Y., Segawa T. and Yabe A., *Proceedings of the 10th International Symposium on Applied Laser Technology Lisbon, Portugal, 2000.*
[16] Usui H., Itoh T. and Saeki T., *Rheol. Acta*, **37** (1998) 122.